THE JOURNAL OF PHYSICAL CHEMISTRY Letters

Letter

Cite This: J. Phys. Chem. Lett. 2019, 10, 352−357

pubs.acs.org/JPCL

Determination of the Solution Structure of Antifreeze Glycoproteins Using Two-Dimensional Infrared Spectroscopy

Giulia Giubertoni,[†] Konrad Meister,[§] Arthur L. DeVries,[‡] and Huib J. Bakker*[,†]

[†]AMOLF, Science Park 104, 1098 XG Amsterdam, The Netherlands

[§]Max-Planck Institute for Polymer Research, D-55128 Mainz, Germany

[‡]University of Illinois at Urbana−Champaign, Urbana, Illinois 61801, United States

Supporting Information

ABSTRACT: We study the solution structure of antifreeze glycoproteins (AFGPs) with linear and two-dimensional infrared spectroscopy (2D-IR). With 2D-IR, we study the coupling between the amide I and amide II vibrations of AFGPs. The measured nonlinear spectral response constitutes a much more clearly resolved amide I spectrum than the linear absorption spectrum of the amide I vibrations and allows us to identify the different structural elements of AFGPs in solution. We find clear evidence for the presence of polyproline II (PPII) helical structures already at room temperature, and we find that the fraction of PPII structures increases when the temperature is decreased to the biological working temperature of AFGP. We observe that inhibition of the antifreeze activity of AFGP using borate buffer or enhancing the antifreeze activity using sulfate buffer does not lead to significant changes in the protein conformation. This finding indicates that AFGPs bind to ice with their sugar side chains.

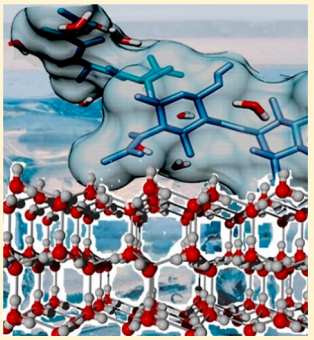

Antifreeze proteins (AFP) and antifreeze glycoproteins (AFGPs) are a unique class of proteins that inhibit the growth of ice crystals in living organisms and thereby enable their survival in freezing and subfreezing habitats.[1,2] AFGPs were the first AFPs to be discovered and are subject to considerably less structural variations than AFPs. The primary structure of an AFGP consists of the repeating tripeptide unit (alanyl−alanyl−threonine) to which a β-D-galactosyl-(1 → 3)-α-*N*-acetyl-D-galactosamine is attached at the threonine side chains, as shown in Figure 1a. AFGPs typically occur in isoforms that are grouped into large $AFGP_{1-5}$ and small $AFGP_{7-8}$ isoforms.

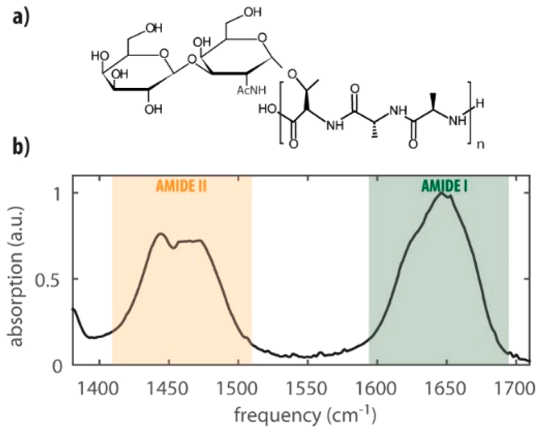

Figure 1. (a) Chemical structure of a representative AFGP repeat; n = 4−50. (b) Infrared spectrum of $AFGP_{1-5}$ at a concentration of 2 wt % in D_2O at room temperature.

The secondary structure of AFGP in solution and at the surface of ice has not yet been unambiguously identified. Early circular dichroism (CD) spectra suggested that AFGPs possess an extended random coil structure in solution.[3] Follow-up studies using a combination of NMR and CD experiments proposed a left-handed helical conformation that is similar to that of a polyproline II (PPII) helix.[4,5] The results of later CD, IR, quasi-elastic light scattering, and Raman spectroscopic studies all suggested the presence of folded structural elements but did not allow a definite determination of the structure.[6] Recently, molecular dynamics simulations and a systematic chemical synthesis study of small AFGP isoforms showed that the sugar unit and the PPII structural element play an important role in the binding to ice.[7,8] The uncertainty regarding the solution structure of AFGPs leaves important questions regarding their working mechanism unanswered. It remains, for instance, unclear which site of the protein binds to ice.

Linear infrared spectroscopy is a widely used method to study the secondary structure of proteins. Structural elements such as α-helixes or β-sheets can be derived from the frequencies of their amide vibrations. In particular, the frequency of the strongly absorbing amide I mode constitutes a clear marker for the presence of specific secondary structural elements.[9,10] Unfortunately, for more complex and (partly) disordered proteins, the measured linear infrared absorption spectra are often too strongly congested to determine the

Received: November 15, 2018
Accepted: January 7, 2019
Published: January 7, 2019

DOI: 10.1021/acs.jpclett.8b03468
J. Phys. Chem. Lett. 2019, 10, 352−357

secondary structure of the protein. Additional information on the protein structure can be obtained with two-dimensional infrared spectroscopy (2D-IR). 2D-IR is a nonlinear spectroscopic technique in which the vibrational response is measured as a function of two frequencies (excitation and probing frequencies). The coupling of different vibrations leads to off-diagonal signals in the 2D-IR spectrum.[11] The magnitude of these off-diagonal signals reflects the strength of the coupling, which can provide information on the relative position and orientation of the vibrations and thereby on the spatial structure of the studied molecule.[12−14]

Here we use 2D-IR to study the coupling between the amide I and amide II modes of AFGPs.[15] We demonstrate that the measurement of this coupling enables decomposition of the complex amide I solution spectrum of AFGP in subbands that correlate with distinct structural elements. Thereby, we can determine the relative fractions of these structural elements of AFGPs in solution as a function of temperature. The spectral decomposition of the amide I spectrum using 2D-IR also allows us to analyze the linear infrared absorption spectrum of the amide I modes and to study the effect of the addition of an enhancer[16] (sulfate) and inhibitor[17,18] (borate) of the antifreeze activity on the structure of AFGPs in solution.

Linear Infrared Absorption Spectrum. Figure 1b shows the normalized infrared spectrum of a solution of $AFGP_{1-5}$ in deuterated water (D_2O), between 1380 and 1720 cm^{-1}. We used a concentration of 2 wt % in all of our experiments as this was the minimum concentration that provided sufficient absorption to perform 2D-IR experiments with a good signal-to-noise. The frequency range between 1400 and 1500 cm^{-1} represents the region of the amide II vibrations, and the frequency range between 1600 and 1700 cm^{-1} represents the amide I region. The amide II vibration is dominated by N−H bending vibrations and the C−N stretching vibrations, whereas the amide I mode is dominated by the stretching of the C═O bond of the amide group. Amide I and amide II modes are strongly coupled by through-bond, mechanical anharmonic interactions.[19]

The AFGP spectrum in the amide II region is congested due to the overlap of modes belonging to different protein conformations and the response of the bending mode of residual HDO in the D_2O solvent.[20] The amide I region is also highly congested and consists of a broad band with a maximum at around 1645 cm^{-1} and a shoulder at around 1620 cm^{-1}. As a result, the different amide I subbands and the corresponding structural motifs of the protein cannot be resolved.

Two-Dimensional Infrared Experiment. We study the vibrational response of the amide I and amide II vibrations and their coupling with 2D-IR spectroscopy. The details of the setup can be found in the literature.[21] In brief, we excite the amide vibrations with a strong femtosecond infrared pulse pair (~100 fs, 4 μJ per pulse). This excitation induces transient absorption changes that are probed with a weaker (0.35 μJ) single-femtosecond probing pulse that is delayed by a time T_w. In all experiments, the excitation pulses are centered at 1630 cm^{-1} with a bandwidth of 200 cm^{-1}, in resonance with the amide I vibrations. The probe pulse is centered at 1630 cm^{-1} to measure the response of the amide I vibrations and at 1450 cm^{-1} to measure the response of the amide II vibrations induced by the excitation of the amide I vibration.

Diagonal Two-Dimensional Infrared Spectra. In the left panel of Figure 2, we show the isotropic 2D-IR spectra obtained by pumping and probing the amide I vibrations (diagonal region)

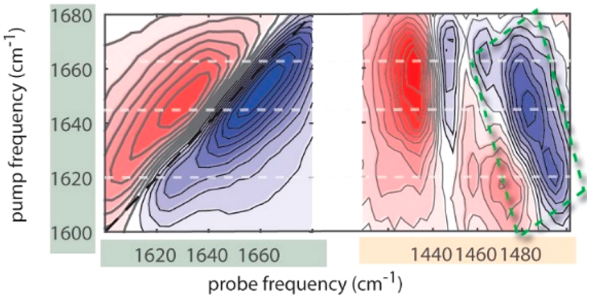

Figure 2. Isotropic 2D-IR spectra of a 2 wt % $AFGP_{1-5}$ solution in D_2O at 0 °C. The spectra were collected at a delay time T_w of 0.5 ps. The left panel shows the 2D-IR spectrum obtained when exciting and probing in the amide I region, and the right panel shows the 2D-IR spectrum obtained when exciting the amide I region and probing the amide II region. Bleaching (reduced absorption) is indicated in blue, while excited-state absorption (increased absorption) is indicated in red.

for a solution of a 2 wt % $AFGP_{1-5}$ solution at 0 °C. The 2D-IR spectrum in the diagonal region shows a clear bleaching component (reduced absorption) due to the depletion of the fundamental ν = 0 to 1 transition and induced ν = 1 to 0 stimulated emission. At a slightly lower probing frequency, we observe an induced ν = 1 to 2 excited-state absorption. The bleaching signal is strongly elongated along the diagonal. The maximum signal is observed at ~1655 cm^{-1}, which is slightly higher than the frequency of the maximum in the linear infrared spectrum. The 2D-IR spectrum also contains a shoulder at 1620 cm^{-1} that has a higher intensity relative to the main band that is observed in the linear infrared spectrum. This difference can be explained from the fact that the signal in the linear infrared spectrum is proportional to $c|\vec{\mu}|^2$, where c is the concentration of the species and $|\vec{\mu}|^2$ is the square of the transition dipole moment of the molecular vibration, whereas the signal of the diagonal 2D-IR spectrum is proportional to $c|\vec{\mu}|^4$. Thus, molecular vibrations with a large transition dipole moment will be enhanced in 2D-IR spectra.[11] It has been shown that the higher nonlinear dependence of the diagonal 2D-IR signal on the transition dipole moment can help in revealing the secondary structure of proteins.[22,23]

Off-Diagonal Two-Dimensional Infrared Spectra. The right panel of Figure 2 shows the isotropic 2D-IR spectrum obtained by exciting the amide I vibrations and probing the amide II vibrations. This region of the 2D-IR spectrum shows the presence of several off-diagonal features or cross-peaks. The cross-peak signals consist of a bleaching component at higher frequencies and an induced absorption component at lower frequencies. This signature implies that the frequency of the probed amide II vibration is shifted to lower frequencies as a result of the excitation of the amide I vibration. At probe frequencies between 1480 and 1500 cm^{-1}, we observe an antidiagonally elongated bleaching band, highlighted by the green rectangle in Figure 2b. In addition, we observe bleaching signals at probe frequencies of 1447 and 1460 cm^{-1} following excitation at ~1660 cm^{-1}. The linear infrared spectrum shows a peak near 1450 cm^{-1} that has been assigned to the CH_3 bending vibration (see Figure S1). Hence, we assign the signal near 1447 cm^{-1} to the coupling of the amide I vibrations and the CH_3 bending mode.[24] To analyze the broad antidiagonal amide II response between 1480 and 1500 cm^{-1}, we plot the

DOI: 10.1021/acs.jpclett.8b03468
J. Phys. Chem. Lett. 2019, 10, 352−357

maximum of this signal as a function of the excitation frequency in the amide I band.

Figure 3a shows the resulting spectra at 0, 5, 23, and 40 °C. We also measured the spectral response at −5 °C, but this

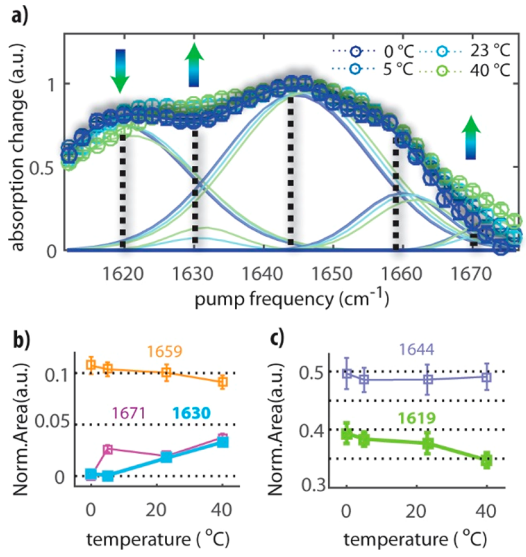

Figure 3. (a) Maximum bleaching signal of the amide I−amide II cross-peak region for probing frequencies between 1480 and 1500 cm^{-1} as a function of the excitation frequency, at four different temperatures, for a solution of AFGP$_{1-5}$ at a concentration of 2%. The signal is normalized to clarify the temperature dependence of the spectra. Also shown are the five Gaussian subbands in which the spectrum is decomposed. (b,c) Areas of the five Gaussian bands used to fit the spectra of (a) as a function of temperature. The areas are normalized to the total area at each temperature. The error bars represent the standard deviations obtained from the global fit and from the propagation of the experimental errors.

spectrum did not show significant changes compared to the off-diagonal 2D-IR spectrum at 0 °C (Figure S3). The spectrum at 0 °C shows a maximum intensity at 1644 cm^{-1} and two shoulders at around 1620 and 1660 cm^{-1}. We find that at higher temperatures a significant change of the spectrum occurs. At 40 °C, the signals at 1630 and 1670 cm^{-1} increase, while the shoulder at 1620 cm^{-1} becomes less pronounced. The measurement of the maximum response of the amide II vibrations as a function of the amide I excitation frequency results in a more clearly structured amide I spectrum compared to the linear IR spectrum of the amide I modes. The improved spectral resolution can be explained from the nonlinear character of the signal. The intensity of the signals measured in the cross-peak region is proportional to the product of the squares of the transition dipole moments of the two coupled molecular modes.[11,15] This leads to a strong suppression of all contributions that do not involve a coupling between amide I and amide II. Hence, all contributions of the background and contaminations that lead to congestion of the linear IR spectrum of the amide I modes are no longer observed in the off-diagonal 2D-IR spectrum, which allows us to identify the different amide I subbands. The resulting spectrum reveals the presence of five different amide I subbands.

We performed a global fit of the spectra at different temperatures using five Gaussian subbands, as shown in Figure 3a. In this fit, we take the widths of the subbands to be temperature-independent, and we assume the central frequencies to blue shift by 0.05 cm^{-1}/ °C to take into account the effect of an increase in temperature on each of the subbands. From the fit, we extract the central frequencies and the temperature-dependent amplitudes of the five subbands. The obtained frequencies agree very well with frequency values reported in previous studies.[25−27] We assign the modes as follows: the 1619 ± 2 cm^{-1} band is assigned to the PPII structure, the 1630 ± 2 cm^{-1} and 1671 ± 2 cm^{-1} bands are assigned to extended structures (or turns), the 1644 ± 3 cm^{-1} band is assigned to a random coil structure, and the 1659 ± 3 cm^{-1} band is assigned to an α-helical conformation. These assignments are in line with previous findings[25−27] and are further supported by the observed polarization dependence of the 2D-IR signals (see the Supporting Information for a complete discussion).

The amide I vibration of the sugar unit *N*-acetyl-D-galactosamine absorbs at 1627 cm^{-1} (see Figure S7) and thus overlaps with the band at 1630 cm^{-1} that is assigned to the amide I vibrations of the protein part of AFGP with an extended conformation.[25−27] However, the observed band for AFGP shows a distinct temperature dependence, which is not observed for the amide I vibration of *N*-acetyl-D-galactosamine (see Figure S7). Hence, the observed band at 1628 cm^{-1} likely contains contributions from both the amide I vibration of *N*-acetyl-D-galactosamine and the amide I vibrations of the protein part of AFGP with an extended conformation.

In Figure 3b,c, we present the normalized areas of the five spectral components as a function of temperature. We find that there is no dominant conformation of AFGP in solution, and at all temperatures, a mixture of different structural elements is present. When the temperature is increased to 40 °C, the amplitude of the PPII band (1619 cm^{-1}) decreases from 0.4 ± 0.02 to 0.35 ± 0.02, while the extended structure bands (1671 and 1630 cm^{-1}) increase from 0 ± 0.01 to 0.04 ± 0.01. The amplitudes of the other two bands show very little change with temperature. We performed the same experiments and data analysis for 2 wt % solutions of AFGP$_{7-8}$ and obtained similar results (Figures S4 and S5).

Comparison of the Linear Infrared Spectra of AFGP$_{1-5}$ and AFGP$_{7-8}$. In Figure 4a, we show linear IR spectra of solutions of AFGP$_{1-5}$ and AFGP$_{7-8}$ in D_2O at room temperature. We observe that AFGP$_{7-8}$ has a stronger absorption in the frequency region between 1580 and 1620 cm^{-1} in comparison to the larger AFGP$_{1-5}$. In comparison to the 2D-IR spectra, these spectra show an additional response near 1595 cm^{-1} due to differences in the amino acid composition.[25,28] For the smaller AFGP$_{7-8}$ isoforms, it was shown that alanine is occasionally substituted by proline in some of the repeated monomer units.[29,30]

The five spectral bands that we obtained from the analysis of the cross-peak region (exciting amide I, probing amide II) of the 2D-IR spectra can now also be used to analyze the linear IR spectra in the amide I region. We decompose the linear IR spectra in these five bands plus a sixth band centered at 1595 cm^{-1}. The center frequencies reported in Figure 3b,c are used as input parameters for the linear IR infrared decomposition. We allow the center frequencies of the six bands to shift slightly to the blue with increasing temperature.[31] The extracted widths and center frequencies are reported in Table S1. Figure 4b shows the linear spectra of solutions of AFGP$_{1-5}$ in D_2O for different temperatures between 5 and 70 °C. We find that the temperature-dependent spectra can be

DOI: 10.1021/acs.jpclett.8b03468
J. Phys. Chem. Lett. 2019, 10, 352−357

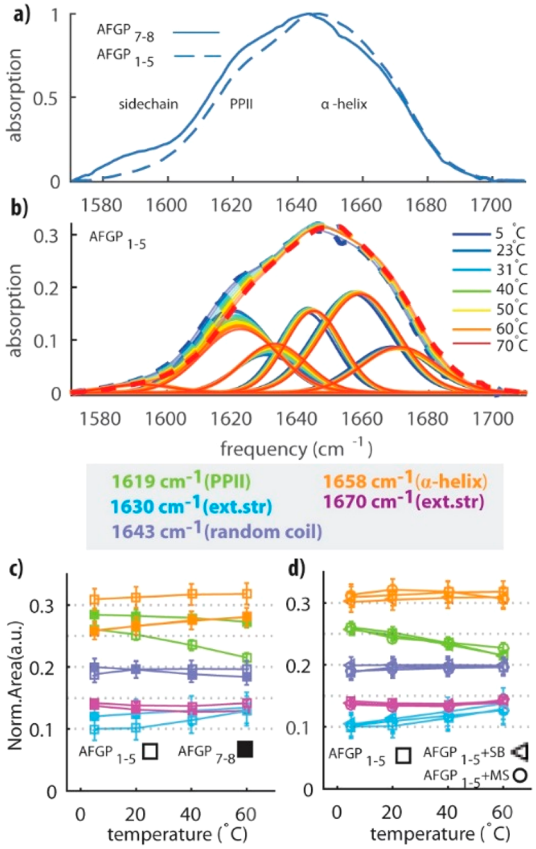

Figure 4. (a) Normalized linear infrared spectra of solutions of $AFGP_{7-8}$ and $AFGP_{1-5}$ at a concentration of ~2 wt % in D_2O at room temperature. (b) Linear infrared spectra of solutions of $AFGP_{1-5}$ at a concentration of ~2 wt % at different temperatures between 5 and 70 °C. We also show the decomposition of the spectra in six Gaussian-shaped bands. (c) Normalized areas of five Gaussian bands that are used to fit the infrared spectra of (b) and the temperature-dependent spectra of $AFGP_{7-8}$ (fit and raw data are reported in Figure S6). (d) Normalized areas of five Gaussian bands that are used to fit the linear spectra of solutions of $AFGP_{1-5}$ (□) and of $AFGP_{1-5}$ in the presence of borate (◁) or in the presence of sufate (○) (Figure S6).

well described with the same bands that we obtained from the 2D-IR measurements.

In Figure 4c, we present the normalized areas of the five bands as a function of temperature. We observe that for all temperatures neither $AFGP_{1-5}$ nor $AFGP_{7-8}$ shows a single dominant conformer, indicating that the proteins have a certain structural flexibility. We find that both $AFGP_{7-8}$ and $AFGP_{1-5}$ have a significant content of PPII structure but that at high temperatures the larger $AFGP_{1-5}$ has less overall PPII content than the shorter $AFGP_{7-8}$. When the temperature is lowered, the PPII content of $AFGP_{1-5}$ increases more strongly than that for $AFGP_{7-8}$ but remains smaller for $AFGP_{1-5}$ than that for $AFGP_{7-8}$ at 5 °C. For both AFGP isoforms, the amplitude of the extended structure band decreases when the temperature is lowered, in agreement with the 2D-IR experiments. Figure 4c also shows that at all temperatures the shorter $AFGP_{7-8}$ isoforms have a lower α-helix content than the larger $AFGP_{1-5}$ isoforms, which likely is a result of their difference in amino acid composition, i.e., $AFGP_{7-8}$ contains more prolines. In fact, proline residues are known to be α-helix breakers.[32] The α-helical content of AFGPs does not show significant changes when the temperature is lowered. We thus find that both AFGP isoforms and, in particular, the larger $AFGP_{1-5}$ tend to form more PPII conformations at the expense of the extended structures as soon as the temperature is lowered to their biological working temperature. This result is in line with a recent molecular dynamics simulation study that showed that PPII structures are important for AFGPs' antifreeze activity.[8]

The antifreeze activity of $AFGP_{7-8}$ is known to be lower than that for $AFGP_{1-5}$,[33,34] which at first sight may be interpreted as a pure size effect, the larger protein showing an energetically more favorable adsorption to the surface of ice. In view of the present findings, the difference in antifreeze activity between $AFGP_{1-5}$ and $AFGP_{7-8}$ may also be partly due to an intrinsic structural difference, the antifreeze activity of $AFGP_{1-5}$ being higher than that of $AFGP_{7-8}$ because of its larger α-helix content. The higher α-helix content could, for instance, be beneficial in the segregation of the hydrophilic and hydrophobic groups of the protein, which is vital for ice binding.

Effect of the Addition of an Enhancer/Inhibitor of the Antifreeze Activity. We measured linear infrared spectra as a function of temperature for solutions of $AFGP_{1-5}$ in D_2O, to which we added 1 M magnesium sulfate or 0.3 M sodium borate.[16,18] Sodium borate is a well-known inhibitor of antifreeze activity, and it has been proposed that borate interacts with AFGP by binding to the *cis*-hydroxyl groups of the β-D-galactopyranosyl group.[18] Magnesium sulfate has been shown to enhance the antifreeze activity of AFGP.[16] The molecular mechanism of this enhancement is unknown. Figure 4d shows the normalized areas of the five different Gaussian-shaped bands obtained from decomposition of the linear spectra (see also Figure S6). We find that at all temperatures the addition of magnesium sulfate or sodium borate does not lead to a significant change in the distribution of structures of $AFGP_{1-5}$ in solution.

Hence, the addition of enhancers or inhibitors does not change the distribution of the protein structural elements and the temperature dependence of this distribution. This result indicates that the effect of the inhibitors and enhancers is likely related to interactions with the disaccharide units, meaning that AFGPs bind to ice with the hydroxyl groups of the disaccharide side chains rather than with the hydrophobic groups of the peptide backbone. This type of binding mechanism agrees with the results of previous studies.[35−38] In one of these studies, the reorientation dynamics of the hydration water of AFGP was investigated, and it was found that inhibiting the antifreeze activity using borate induced no changes in the dynamics of the water molecules.[36] This result indicated that borate is primarily interacting with the sugar unit of AFGP, in agreement with the present results.

We used linear IR and 2D-IR to study the structure of different AFGP isoforms in solution. With 2D-IR, we measured the spectral response of the amide II modes dependent on the excitation frequency of the amide I modes. The obtained response constitutes a much more clearly structured amide I spectrum than the linear IR spectrum. This better resolution can be explained from the nonlinear character of the signal that leads to suppression of background and/or contamination signals that congest the linear amide I spectrum. The amide II−amide I cross-peak response reveals the presence of five distinct amide I vibrations, which we used to decompose and analyze the linear infrared amide I spectra of $AFGP_{1-5}$ and $AFGP_{7-8}$. We assigned the 1619 cm^{-1} band to a PPII structure,

DOI: 10.1021/acs.jpclett.8b03468
J. Phys. Chem. Lett. 2019, 10, 352−357

the 1630 and 1670 cm^{-1} bands to an extended structure (or turn), the 1644 cm^{-1} band to a random coil structure, and the 1659 cm^{-1} band to an α-helix.

We found that AFGPs already adopt a PPII conformation at room temperature. This PPII content increases as the temperature is lowered. We further observed that the addition of borate, as an inhibitor of antifreeze activity, or sulfate, as an enhancer of antifreeze activity, has a negligible effect on the distribution of AFGP structures in solution. This result indicates that the AFGPs bind to ice with the hydroxyl groups of their disaccharide side chains.

Using linear and 2D-IR spectroscopy, we thus identifed the different structural motifs and conformations of AFGPs in aqueous solution. Our results demonstrate that AFGPs do not have one preferred secondary structure and have a high structural flexibility, which make them quite distinct from nonglycosylated AFPs that typically have one preferred conformation and are very rigid.[39,40]

■ ASSOCIATED CONTENT

Supporting Information

The Supporting Information is available free of charge on the ACS Publications website at DOI: 10.1021/acs.jpclett.8b03468.

Experimental methods; linear infrared and 2DIR spectra of $AFGP_{7-8}$; linear infrared of $AFGP_{1-5}$ in 0.3 M sodium borate and 1 M magnesium sulfate; and linear infrared of *N*-acetyl-D-galactosamine (PDF)

■ AUTHOR INFORMATION

Corresponding Author

*E-mail: H.Bakker@amolf.nl.

ORCID

Giulia Giubertoni: 0000-0002-3417-4987

Konrad Meister: 0000-0002-6853-6325

Huib J. Bakker: 0000-0003-1564-5314

Notes

The authors declare no competing financial interest.

■ ACKNOWLEDGMENTS

This work is part of the industrial partnership programme Hybrid Soft Materials that is carried out under an agreement between Unilever Research and The Netherlands Organisation for Scientific Research (NWO).

■ REFERENCES

(1) DeVries, A. L.; Wohlschlag, D. E. Freezing Resistance in Some Antarctic Fishes. *Science (Washington, DC, U. S.)* **1969**, *163*, 1073−1075.

(2) Duman, J. G. Antifreeze and Ice Nucleator Proteins in Terrestrial Arthropods. *Annu. Rev. Physiol.* **2001**, *63*, 327−357.

(3) Franks, F.; Morris, E. R. Blood Glycoprotein from Antarctic Fish. Possible Conformational Origin of Antifreeze Activity. *Biochim. Biophys. Acta, Gen. Subj.* **1978**, *540*, 346−356.

(4) Bush, C. A.; Feeney, R. E. Conformation of the Glycotripeptide Repeating Unit of Antifreeze Glycoprotein of Polar Fish as Determined from the Fully Assigned Proton n.m.r. Spectrum. *Int. J. Pept. Protein Res.* **1986**, *28*, 386−397.

(5) Bush, C. A.; Feeney, R. E.; Osuga, D. T.; Ralapati, S.; Yeh, Y. Antifreeze Glycoprotein. Conformational Model Based on Vacuum Ultraviolet Circular Dichroism Data. *Int. J. Pept. Protein Res.* **1981**, *17*, 125−129.

(6) Yeh, Y.; Feeney, R. E. Antifreeze Proteins: Structures and Mechanisms of Function. *Chem. Rev.* **1996**, *96*, 601−618.

(7) Tachibana, Y.; Fletcher, G. L.; Fujitani, N.; Tsuda, S.; Monde, K.; Nishimura, S. I. Antifreeze Glycoproteins: Elucidation of the Structural Motifs That Are Essential for Antifreeze Activity. *Angew. Chem., Int. Ed.* **2004**, *43*, 856−862.

(8) Mochizuki, K.; Molinero, V. Antifreeze Glycoproteins Bind Reversibly to Ice via Hydrophobic Groups. *J. Am. Chem. Soc.* **2018**, *140*, 4803−4811.

(9) Krimm, B. S.; Bandekar, J. Vibrational Spectroscopy and Conformation. *Adv. Protein Chem.* **1986**, *38*, 48109.

(10) Barth, A.; Zscherp, C. What Vibrations Tell Us about Proteins. *Q. Rev. Biophys.* **2002**, *35*, 369−430.

(11) Hamm, P.; Zanni, M. G. *Concepts and Methods of 2D Infrared Spectroscopy*; Cambridge University Press: Cambridge, U.K., 2011.

(12) Zhang, T. O.; Alperstein, A. M.; Zanni, M. T. Amyloid β-Sheet Secondary Structure Identified in UV-Induced Cataracts of Porcine Lenses Using 2D IR Spectroscopy. *J. Mol. Biol.* **2017**, *429*, 1705−1721.

(13) Dutta, B.; Vos, B. E.; Rezus, Y. L. A.; Koenderink, G. H.; Bakker, H. J. Observation of Ultrafast Vibrational Energy Transfer in Fibrinogen and Fibrin Fibers. *J. Phys. Chem. B* **2018**, *122*, 5870−5876.

(14) Petti, M. K.; Lomont, J. P.; Maj, M.; Zanni, M. T. Two-Dimensional Spectroscopy Is Being Used to Address Core Scientific Questions in Biology and Materials Science. *J. Phys. Chem. B* **2018**, *122*, 1771−1780.

(15) Deflores, L. P.; Ganim, Z.; Nicodemus, R. A.; Tokmakoff, A. Amide I′-II′ 2D IR Spectroscopy Provides Enhanced Protein Secondary Structural Sensitivity. *J. Am. Chem. Soc.* **2009**, *131*, 3385−3391.

(16) Meister, K.; Duman, J. G.; Xu, Y.; DeVries, A. L.; Leitner, D. M.; Havenith, M. The Role of Sulfates on Antifreeze Protein Activity. *J. Phys. Chem. B* **2014**, *118*, 7920−7924.

(17) Ebbinghaus, S.; Meister, K.; Born, B.; DeVries, A. L.; Gruebele, M.; Havenith, M. Antifreeze Glycoprotein Activity Correlates with Long-Range Protein−Water Dynamics. *J. Am. Chem. Soc.* **2010**, *132*, 12210−12211.

(18) Ahmed, A. I.; Yeh, Y.; Osuga, Y. Y.; Feeney, R. E. Antifreeze Glycoproteins from Antarctic Fish. Inactivation by Borate. *J. Biol. Chem.* **1976**, *251*, 3033−3036.

(19) DeFlores, L. P.; Ganim, Z.; Ackley, S. F.; Chung, H. S.; Tokmakoff, A. The Anharmonic Vibrational Potential and Relaxation Pathways of the Amide I and II Modes of N-Methylacetamide. *J. Phys. Chem. B* **2006**, *110*, 18973−18980.

(20) Bodis, P.; Larsen, O. F. A.; Woutersen, S. Vibrational Relaxation of the Bending Mode of HDO in Liquid D2O. *J. Phys. Chem. A* **2005**, *109*, 5303−5306.

(21) Selig, O.; Siffels, R.; Rezus, Y. L. A. Ultrasensitive Ultrafast Vibrational Spectroscopy Employing the Near Field of Gold Nanoantennas. *Phys. Rev. Lett.* **2015**, *114*, 233004.

(22) Dunkelberger, E. B.; Grechko, M.; Zanni, M. T. Transition Dipoles from 1D and 2D Infrared Spectroscopy Help Reveal the Secondary Structures of Proteins: Application to Amyloids. *J. Phys. Chem. B* **2015**, *119*, 14065−14075.

(23) Grechko, M.; Zanni, M. T. Quantification of Transition Dipole Strengths Using 1D and 2D Spectroscopy for the Identification of Molecular Structures via Exciton Delocalization: Application to α-Helices. *J. Chem. Phys.* **2012**, *137*, 184202.

(24) Barth, A. The Infrared Absorption of Amino Acid Side Chains. *Prog. Biophys. Mol. Biol.* **2000**, *74*, 141−173.

(25) Tsvetkova, N. M.; Phillips, B. L.; Krishnan, V. V.; Feeney, R. E.; Fink, W. H.; Crowe, J. H.; Risbud, S. H.; Tablin, F.; Yeh, Y. Dynamics of Antifreeze Glycoproteins in the Presence of Ice. *Biophys. J.* **2002**, *82*, 464−473.

(26) Lane, A. N.; Hays, L. M.; Tsvetkova, N.; Feeney, R. E.; Crowe, L. M.; Crowe, J. H. Comparison of the Solution Conformation and Dynamics of Antifreeze Glycoproteins from Antarctic Fish. *Biophys. J.* **2000**, *78*, 3195−3207.

DOI: 10.1021/acs.jpclett.8b03468
J. Phys. Chem. Lett. 2019, 10, 352−357

(27) Drewes, J. A.; Rowlen, K. L. Evidence for a Gamma-Turn Motif in Antifreeze Glycopeptides. *Biophys. J.* **1993**, *65*, 985−991.
(28) Chirgadze, Y. N.; Fedorov, O. V.; Trushina, N. P. Estimation of Amino Acid Residue Side-chain Absorption in the Infrared Spectra of Protein Solutions in Heavy Water. *Biopolymers* **1975**, *14*, 679−694.
(29) Ananthanarayanan, V. S.; Slaughter, D.; Hew, C. L. Antifreeze Proteins from the Ocean Pout, Macrozoarces Americanus: Circular Dichroism Spectral Studies on the Native and Denatured States. *Biochim. Biophys. Acta, Protein Struct. Mol. Enzymol.* **1986**, *870*, 154−159.
(30) Lin, Y.; Duman, J. G.; DeVries, A. L. Studies on the Structure and Activity of Low Molecular Weight Glycoproteins from an Antarctic Fish. *Biochem. Biophys. Res. Commun.* **1972**, *46*, 87−92.
(31) Amunson, K. E.; Kubelka, J. On the Temperature Dependence of Amide I Frequencies of Peptides in Solution. *J. Phys. Chem. B* **2007**, *111*, 9993−9998.
(32) Jacob, J.; Duclohier, H.; Cafiso, D. S. The Role of Proline and Glycine in Determining the Backbone Flexibility of a Channel-Forming Peptide. *Biophys. J.* **1999**, *76*, 1367−1376.
(33) Burcham, T. S.; Knauf, M. J.; Osuga, D. T.; Feeney, R. E.; Yeh, Y. Antifreeze Glycoproteins: Influence of Polymer Length and Ice Crystal Habit on Activity. *Biopolymers* **1984**, *23*, 1379−1395.
(34) DeVries, A. L. The Role of Antifreeze Glycopeptides and Peptides in the Freezing Avoidance of Antarctic Fishes. *Comp. Biochem. Physiol. – Part B Biochem.* **1988**, *90*, 611−621.
(35) Meister, K.; Devries, A. L.; Bakker, H. J.; Drori, R. Antifreeze Glycoproteins Bind Irreversibly to Ice. *J. Am. Chem. Soc.* **2018**, *140*, 9365−9368.
(36) Groot, C. C. M.; Meister, K.; Devries, A. L.; Bakker, H. J. Dynamics of the Hydration Water of Antifreeze Glycoproteins. *J. Phys. Chem. Lett.* **2016**, *7*, 4836−4840.
(37) DeVries, A. L. Glycoproteins as Biological Antifreeze Agents in Antarctic Fishes. *Science (Washington, DC, U. S.)* **1971**, *172*, 1152−1155.
(38) Knight, C. A.; Driggers, E.; DeVries, A. L. Adsorption to Ice of Fish Antifreeze Glycopeptides 7 and 8. *Biophys. J.* **1993**, *64*, 252−259.
(39) Liou, Y.-C.; Tocilj, A.; Davies, P. L.; Jia, Z. Mimicry of Ice Structure by Surface Hydroxyls and Water of a β-Helix Antifreeze Protein. *Nature* **2000**, *406*, 322−324.
(40) Sicheri, F.; Yang, D. S. C. Ice-Binding Structure and Mechanism of an Antifreeze Protein from Winter Flounder. *Nature* **1995**, *375*, 427−431.

DOI: 10.1021/acs.jpclett.8b03468
J. Phys. Chem. Lett. 2019, 10, 352−357